A Study on the Influence of Plasma Nitriding Technology Parameters on the Working Surface Deformation of Hypoid Gears

Le Hong Ky
Vinh Long University of Technology Education
Vinh Long, Vietnam
kylh@vlute.edu.vn

Received: 23 September 2022 | Revised: 15 October 2022 | Accepted: 17 October 2022

Abstract-This paper presents the results of the research on the influence of plasma nitriding technology parameters on the working surface deformation of hypoid gears. Blue light technology with non-contact measuring devices is used to determine the working surface deformation of hypoid gears after plasma nitriding. The study has determined a regression equation showing the influence of plasma nitriding technology parameters on the deformation of the working surface of the hypoid gear. The minimum deformation optimization value at the planning area is 0.0071746 at permeation temperature *TL*=4.89^{o}C, permeation time *h*=510h, and gas flow 1 *G1*=6.02L/h.

Keywords-hypoid gear; surface deformation; computer aided verification; plasma nitriding

I. INTRODUCTION

The hypoid gear pair has some special features: the axes of the gears are diagonal, the average helix angle of the active gear and the passive gear are not equal, and the tangential module of the active gear is larger than those of the passive gear. The constraining forces at the contact trace acting on the active and passive gears are equal, but the tangential forces are not equal [1]. Hypoid gears are shaped by milling [2] (Figure 1(a)). This study uses plasma nitriding to improve the working surface quality of hypoid gears. Plasma nitriding is an advanced and environmentally friendly technology that is very effective for products with simple structures. The advantage of this technology is that it can control the white layer, so it is very suitable for impregnating products that require high quality. The disadvantage of the plasma nitriding method is the occurrence of plasma amplification during the penetration of the surface. This disadvantage can be completely eliminated by controlling the plasma thickness [3, 4]. Plasma nitriding is the process of alloying the surface with nitrogen. The permeation process is carried out in a vacuum furnace at low pressure with a mixture of H_2, N_2, CH_4, and Ar gases [3, 4]. Under high voltage, the gases are ionized, creating a plasma flow. Nitrogen ions are accelerated during plasma collision with the sample. This ion bombardment process heats, cleans and forms a hard layer with good wear resistance, increasing fatigue strength [5].

The ELTROPUL permeation furnace [6] uses a pre-generated plasma pulse source. It creates stable plasma under all circumstances, permeates parts with complex geometries, lowers temperatures providing for the lowest permeation and the most treated surfaces. The surface layer that is nitrified after ion nitriding is a thin, solid white layer outside and a diffuse domain inside. The properties of the surface layer (deformation, hardness, roughness, cleanliness), permeation layer depth, permeation layer properties, microscopic hardness of the material, etc. are influenced by input parameters such as voltage, current density, permeation time, permeation temperature, compositions of gas mixture, gas pressure, etc. Authors in [7] used plasma nitriding treatment to reduce wear occurring in hot forging applications, but there is a need for further optimization of the processes to achieve suitable properties for different loaded forging tools. This work presents the influence of the main process parameters on the wear properties of the mold. The effects of nitriding parameters such as temperature, nitrogen flow, and time on nitriding depth, hardness, and crack sensitivity were investigated. Authors in [8] studied the surface properties of the Fe_4N layer on steel modified by pulsed plasma nitriding [8]. Authors in [9] studied the phase structure and surface hardness value of AISI H13 ion nitrided steel under different temperatures. Authors in [10] worked on nitriding of tertiary alloys based on iron (Fe-Cr-Ti and Fe-Cr-Al) and other alloy steels [10]. There have been many studies on the mechanical properties of steel after plasma nitriding [9-11]. To the best of our knowledge, there are no studies that consider plasma nitriding of hypoid gears made of 18ХГТ alloy steel.

Precision inspection has been widely used in manufacturing to measure the dimensional accuracy of parts and products to meet the quality requirements. For regular geometric features, coordinate-measuring machines can be used effectively to assess the accuracy and tolerances. For parts with free-form surfaces, the inspection becomes complex. Therefore, numerous researches have been carried out to tackle both fundamental and application issues concerning free-form surface inspection. In addition to academic research, some commercial packages have also been developed [12]. This

Corresponding author: Le Hong Ky

study used ATOS's non-contact measuring instrument to collect point cloud data of samples before and after plasma nitriding. The evaluation of surface deviations is handled by GOM software, also of ATOS. This application has never been used before with hypoid gear working surfaces.

II. PLASMA NITRIDING FOR HYPOID GEAR SAMPLES

A. Experimental Samples

The plasma nitriding sample consists of passive gear teeth, which have been machined from 18ХГТ and improved to a uniform hardness of 34 – 36 HRC (Figure 1). Each tooth is cut separately by wire cutting. The teeth are marked in order from 1 to 41 corresponding to the total number of teeth of the gear, as shown in Figure 1(b).

(a) (b)

Fig. 1. Sample preparation for the experiment: (a) Passive hypoid gear, (b) teeth that are cut apart.

B. Experiment Planning

1) Selection of Input Parameters

H4580 Eltrolab is used to perform plasma nitriding. Many parameters affect the surface quality [13]:

h is the number of hours executed in each step of the program (h), *m* is the number of minutes executed in each step of the program (min), *P* is the pressure (Pa), *TL* the permeation temperature (^oC), *TG* the detailed temperature rising rate over time (^oC/min), *TW* the furnace wall temperature (^oC), *WG* the furnace wall temperature rising rate over time (^oC/min), *V* is the Voltage (V), *PD* the Pulse Duration (μs), *PR* the number of repetitions of the pulse, and *G1-G4* are gas flows 1-4 respectively (l/h).

In reality, in permeation with samples of the same material and size with little change, the voltage *V* and pressure *P* are fixed. Detailed temperature rising rate over time *TG*, furnace wall temperature *TW*, and furnace wall temperature rising rate over time *WG* depend on *TL* and h. *G1-G4* are proportional to each other [14]. According to the requirements for selecting input factors, the experimental variables were selected including *TL*, *h*, and *G1*. The remaining factors remain unchanged. The influence relationship of plasma nitriding technology parameters on the deformation of the working surface of hypoid gears is:

$$\varepsilon = f(h, TL, G1) \quad (1)$$

where ε is the absolute deviation due to thermal deformation of tooth working surface (mm).

2) The Permeation Process

When the power supply is closed under high voltage and low pressure, the first heating process, until reaching a temperature of 250-300^{o}C, passes through the surface activation stage, followed by the second heating stage until reaching the permeation temperature (510-550^{o}C). The end of the permeation period, lasting from 4 to 8h (depending on the installation program), is the automatic cooling phase.

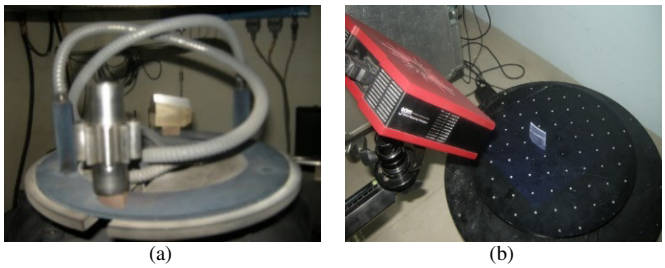

(a) (b)

Fig. 2. Plasma nitriding of hypoid gear tooth samples annd scanning of samples after permeation. (a) Samples in the permeation furnace, (b) measuring and scanning of samples after permeation.

3) The Conduct of Permeation of the Test Samples

Level 2 planning with 27 experiments and programming to control the permeation process on H4580 Eltrolab are shown in Table I. Plasma nitriding of hypoid gear tooth samples was carried out as shown in Figure 2(a).

4) Test Samples Measuring and Scanning

One of the development applications of the technique is non-contact measurement using Computer Aided Verification (CAV) to determine the deformation of the surface. Here, deformation is understood as the differences from the origin (standard). The basic CAV steps include data collection (point cloud) from the original object, data after machining (here, after permeation), superposition of 2 cloud data according to predetermined standards, and deviation evaluation.

In this study, Capture 3D–ATOS Blue Light III TRIPLE non-contact measuring device with blue light technology were used to collect point cloud data of samples before and after plasma nitriding, as shown in Figure 2(b).

III. RESULTS AND DISCUSSION

After loading the sample point cloud data before and after permeating into the software and superimposing these two data sets, automatic comparison was made with the two tooth surface point cloud data, displaying the measurement results of deviation due to deformation on the tooth surfaces of each test sample as shown in Figure 3. The software produces a statistical report on the measurement results of deviation due to deformation at specified points on the gear tooth surface of each measured sample. The deviation due to surface deformation of each measured sample is the average value of the specified points on the gear tooth surface. Measurement results with 27 samples are summarized in Table II.

TABLE I. CONTROL PROGRAM OF THE PERMEATION PROCESS

Ps	*h*	*m*	*Opt*	*P*	*TL*	*TG*	*TW*	*WG*	*V*	*PD*	*PR*	*G1*	*G2*	*G3*	*G4*
1	4	2	144	250	510	10	530	10	470	50	100	4	12	0	0
2	4	2	144	250	510	10	530	10	470	50	100	6	18	0	0
3	4	2	144	250	510	10	530	10	470	50	100	8	24	0	0
4	4	2	144	250	530	10	530	10	470	50	100	4	12	0	0
5	4	2	144	250	530	10	530	10	470	50	100	6	18	0	0
6	4	2	144	250	530	10	530	10	470	50	100	8	24	0	0
7	4	2	144	250	550	10	530	10	470	50	100	4	12	0	0
8	4	2	144	250	550	10	530	10	470	50	100	6	18	0	0
9	4	2	144	250	550	10	530	10	470	50	100	8	24	0	0
10	6	2	144	250	510	10	530	10	470	50	100	4	12	0	0
11	6	2	144	250	510	10	530	10	470	50	100	6	18	0	0
12	6	2	144	250	510	10	530	10	470	50	100	8	24	0	0
13	6	2	144	250	530	10	530	10	470	50	100	4	12	0	0
14	6	2	144	250	530	10	530	10	470	50	100	6	18	0	0
15	6	2	144	250	530	10	530	10	470	50	100	8	24	0	0
16	6	2	144	250	550	10	530	10	470	50	100	4	12	0	0
17	6	2	144	250	550	10	530	10	470	50	100	6	18	0	0
18	6	2	144	250	550	10	530	10	470	50	100	8	24	0	0
19	8	2	144	250	510	10	530	10	470	50	100	4	12	0	0
20	8	2	144	250	510	10	530	10	470	50	100	6	18	0	0
21	8	2	144	250	510	10	530	10	470	50	100	8	24	0	0
22	8	2	144	250	530	10	530	10	470	50	100	4	12	0	0
23	8	2	144	250	530	10	530	10	470	50	100	6	18	0	0
24	8	2	144	250	530	10	530	10	470	50	100	8	24	0	0
25	8	2	144	250	550	10	530	10	470	50	100	4	12	0	0
26	8	2	144	250	550	10	530	10	470	50	100	6	18	0	0
27	8	2	144	250	550	10	530	10	470	50	100	8	24	0	0

TABLE II. SYNTHESIS OF THE DEVIATION MEASUREMENT RESULTS DUE TO THERMAL DEFORMATION OF WORK SURFACE

Trial	*TL* (°C)	*h* (h)	*G1* (L/h)	$\mathcal{E}$ (mm)
1	4	510	4	0.0080
2	4	510	6	0.0071
3	4	510	8	0.0082
4	4	530	4	0.0086
5	4	530	6	0.0085
6	4	530	8	0.0093
7	4	550	4	0.0103
8	4	550	6	0.0099
9	4	550	8	0.0114
10	6	510	4	0.0082
11	6	510	6	0.0078
12	6	510	8	0.0080
13	6	530	4	0.0090
14	6	530	6	0.0083
15	6	530	8	0.0092
16	6	550	4	0.0105
17	6	550	6	0.0099
18	6	550	8	0.0111
19	8	510	4	0.0096
20	8	510	6	0.0087
21	8	510	8	0.0098
22	8	530	4	0.0099
23	8	530	6	0.0099
24	8	530	8	0.0101
25	8	550	4	0.0119
26	8	550	6	0.0111
27	8	550	8	0.0139

1) Influence of Input Parameters on Surface Deformation

The experimental results (Table III) were processed using Minitab software and were preliminarily analyzed [15, 16].

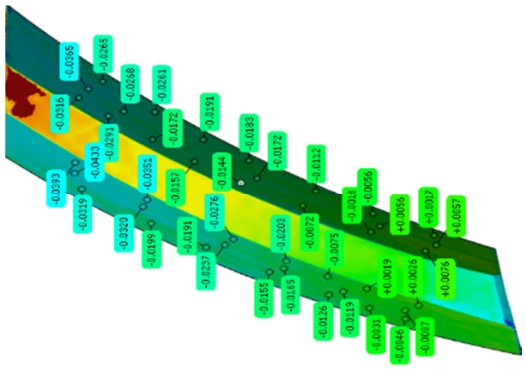

Fig. 3. Measurement result display on two gear tooth surfaces.

TABLE III. EXPERIMENTAL RESULTS ANALYSIS

Term	Coef	SE Coef	T-Value	P-Value	VIF
Constant	0.008207	0.000194	42.36	0.000	
TL	0.000756	0.000090	8.42	0.000	1.00
h	0.001367	0.000090	15.24	0.000	1.00
G1	0.000278	0.000090	3.10	0.007	1.00
TL×*TL*	0.000678	0.000155	4.36	0.000	1.00
h×*h*	0.000544	0.000155	3.50	0.003	1.00
G1×*G1*	0.000811	0.000155	5.22	0.000	1.00
TL×*h*	0.000042	0.000110	0.38	0.709	1.00
TL×*G1*	0.000033	0.000110	0.30	0.765	1.00
h×*G1*	0.000292	0.000110	2.66	0.017	1.00

It was found that there were some coefficients with p-value greater than the precision a=0.05, so these coefficients were discarded, and the experimental results were reanalyzed (Table IV).

TABLE IV. EXPERIMENTAL RESULTS SECOND ANALYSIS

Term	Coef	SE Coef	T-Value	P-Value	VIF
Constant	0.008207	0.000185	44.48	0.000	
TL	0.000756	0.000085	8.85	0.000	1.00
h	0.001367	0.000085	16.00	0.000	1.00
G1	0.000278	0.000085	3.25	0.004	1.00
TL×TL	0.000678	0.000148	4.58	0.000	1.00
h×h	0.000544	0.000148	3.68	0.002	1.00
G1×G1	0.000811	0.000148	5.48	0.000	1.00
h×G1	0.000292	0.000105	2.79	0.012	1.00

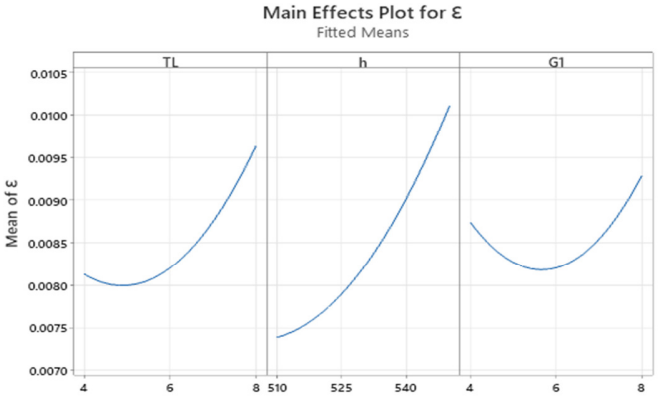

Fig. 4. The influence of input parameters (*TL, h, G1*) on surface deformation (*Ɛ*).

The influence of the input parameters on the surface deformation is presented in Figure 4. Corresponding to the three levels (-1), (0), and (+1) of each factor, the software calculates the average value of the output response and displays it as a point (Figure 4). From there, to find out the parameter that has the most influence on the output value, it is possible to make a brief comment on the influence of the input parameters on the surface deformation. With the permeation temperature *TL*, the influence on the output is parabolic, with the minimum near the value 0, and the influence chart goes from a minimum of about 0.0080 to the maximum value of 0.0095 at the value area +1 of the planning. For permeation time *h*, the influence on the output is parabolic, with the minimum near the value 0 and the influence chart goes from the minimum value around 0.0075 towards the maximum value of 0.0100 at the value area +1 of the planning. With a gas permeation concentration of 1 *G1*, the influence on the output is parabolic, with the minimum near the value 0 and the influence chart goes from about 0.0085 to a minimum and to the maximum value of 0.0095 at the value area +1 of the planning.

With the Pareto chart in Figure 5, it is found that the parameters that greatly affect the surface deformation are *h* and *TL*. These parameters interact at level 2 of *G1*. In the standard distribution chart in Figure 6, the effect parameters are standardized. These are the parameters that affect the regression equation.

2) Regression Equation of Experimental Data

The variance (ANOVA) of the regression equation for the output object is analyzed, with the selection of removing the parameters that do not affect the determined regression equation (Table V) [17]. The variance analysis table has all p-Values less than 0.05. This shows that these parameters all have an influence on the regression equation.

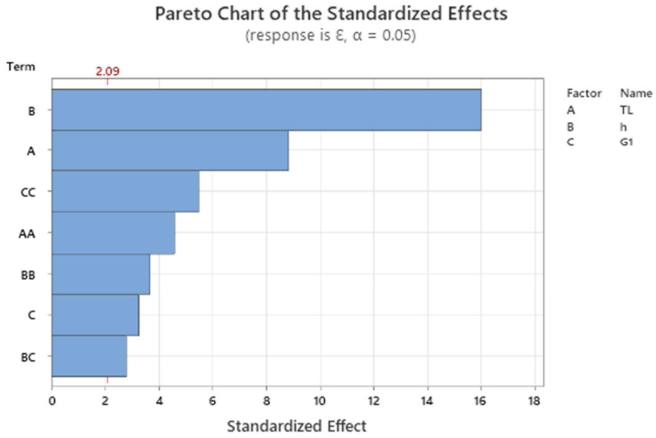

Fig. 5. Pareto chart of input parameters.

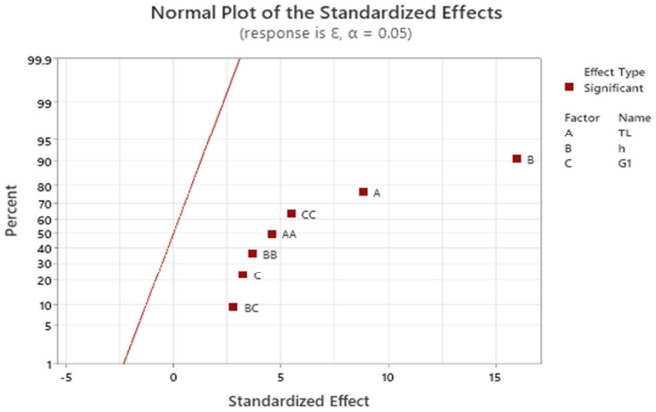

Fig. 6. Standard distribution chart of the standardized effect parameters.

TABLE V. ANALYSIS OF VARIANCE

Source	DF	Adj SS	Adj MS	F-Value	P-Value
Model	7	0.000055	0.000008	59.59	0.000
Linear	3	0.000045	0.000015	114.93	0.000
TL	1	0.000010	0.000010	78.24	0.000
h	1	0.000034	0.000034	255.98	0.000
G1	1	0.000001	0.000001	10.57	0.004
Square	3	0.000008	0.000003	21.53	0.000
TL×TL	1	0.000003	0.000003	20.99	0.000
h×h	1	0.000002	0.000002	13.54	0.002
G1×G1	1	0.000004	0.000004	30.05	0.000
2-Way Interaction	1	0.000001	0.000001	7.77	0.012
h×G1	1	0.000001	0.000001	7.77	0.012
Error	19	0.000002	0.000000		
Total	26	0.000057			

The suitability of the data was evaluated using a set of R^2, adjusted R^2, and predicted R^2 parameters. These parameters all have a value bigger than 90%, which means that the regression equation is completely consistent with the experimental data.

TABLE VI. SUITABILITY

S	R^2	R^2(adj)	R^2(pred)
0.0003624	95.64%	94.04%	91.01%

Then the general equation (1) is rewritten as a regression equation in natural form:

$$\begin{aligned}\varepsilon = 0.388 &- 0.001656\,TL - 0.001418\,h \\ &- 0.00616\,G1 + 0.000169\,TL^2 \\ &+ 0.000001\,h^2 + 0.000203\,G1^2 \\ &+ 0.000007\,h \times G1\end{aligned} \quad (2)$$

The chart in Figure 7 shows the domain of double interactions between the parameters. Based on these charts, the changing trend of surface deformation can be seen when changing separately the two parameters shown in each chart.

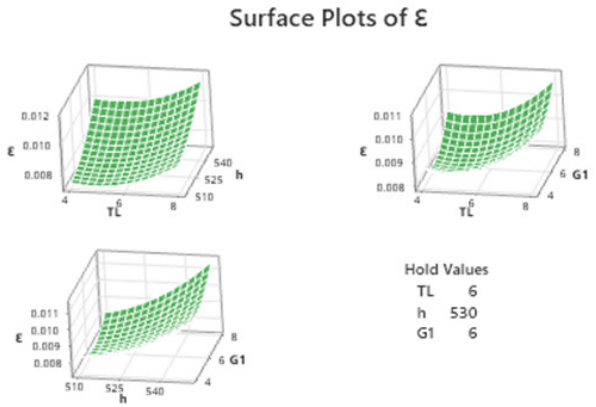

Fig. 7. Interaction charts between parameters.

3) Optimization of Permeation Technology Parameters

With the regression equation found, minimum deformation optimization is carried out with the following contour conditions:

$$\min \varepsilon: \begin{cases} 4 \le TL \le 8 \\ 510 \le h \le 550 \\ 4 \le G1 \le 8 \end{cases}$$

Minitab software gives the optimization results shown in Table VII:

TABLE VII. MINITABL RESULTS

TL	*h*	*G1*	Ɛ Fit
4.89	510	6.02	0.0071746

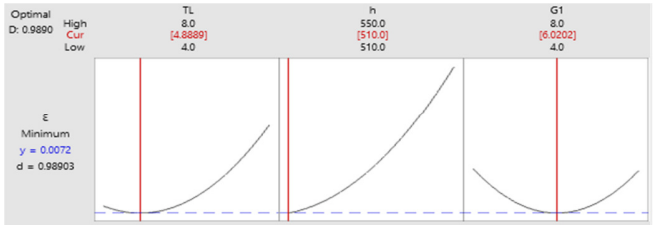

Fig. 8. Software result of minimizing deformation in the planning area.

IV. CONCLUSION

Blue light technology with a non-contact measuring device is used to determine the working surface deformation of hypoid gears after plasma nitriding. The current study has determined the regression equation showing the influence of plasma nitriding technology parameters on surface deformation. Research results show that the parameters of plasma nitriding technology that have a great influence on surface deformation are permeation time *h* and permeation temperature *TL*. The gas permeation concentration 1 *G1* has little effect on the surface deformation and the level 2 interaction with *h* and *TL*. The minimum deformation optimization value in the planning area is 0.0071746 for *TL*=4.89°C, *h*=510h, and *G1*= 6.02L/h. Thus, the working surface deformation of hypoid gears after permeation is very little influenced by plasma nitriding technology parameters.

To the best of our knowledge, plasma nitriding of hypoid gears along with the use of blue light technology with non-contact gauges to determine the gear working surface deformation have not been studied before. With the technological parameters determined as above, it is possible to proceed to set up the hypoid gear plasma nitriding technology process in industrial production.

REFERENCES

[1] M. Kolivand, *Development of Tooth Contact and Mechanical Efficiency Models for Face-milled and Face-hobbed Hypoid and Spiral Bevel Gears*. Columbus, OH, USA: Ohio State University, 2009.

[2] T. H. Le, V. B. Pham, and T. D. Hoang, "Surface Finish Comparison of Dry and Coolant Fluid High-Speed Milling of JIS SDK61 Mould Steel," *Engineering, Technology & Applied Science Research*, vol. 12, no. 1, pp. 8023–8028, Feb. 2022, https://doi.org/10.48084/etasr.4594.

[3] D. Pye, *Practical Nitriding and Ferritic Nitrocarburizing*. ASM International, 2003.

[4] *ISO/TR 22849:2011(en), Design recommendations for bevel gears*. ISO, 2011.

[5] D. Y. Chung, H. J. Kim, and H. N. Kim, "A Study on the Erosion Characteristics of the Micropulsed Plasma Nitrided Barrel of a Rifle," in *19th International Symposium of Ballistics*, Interlaken, Switzerland, May 2001.

[6] U. Huchel, S. Strämke, and J. Cockrem, "Pulsed Plasma Nitriding of Tools." ELTRO GmbH.

[7] H. Paschke, M. Weber, G. Braeuer, T. Yilkiran, B.-A. Behrens, and H. Brand, "Optimized plasma nitriding processes for efficient wear reduction of forging dies," *Archives of Civil and Mechanical Engineering*, vol. 12, no. 4, pp. 407–412, Dec. 2012, https://doi.org/10.1016/j.acme.2012.06.001.

[8] J. C. Díaz-Guillén *et al.*, "Surface Properties of Fe4N Compounds Layer on AISI 4340 Steel Modified by Pulsed Plasma Nitriding," *Journal of Materials Science & Technology*, vol. 29, no. 3, pp. 287–290, Mar. 2013, https://doi.org/10.1016/j.jmst.2013.01.017.

[9] M. R. Cruz and M. H. Staia, "Ion nitrided AISI H13 tool steel Part 2 – High temperature performance under sliding wear conditions," *Surface Engineering*, vol. 22, no. 5, pp. 367–374, Oct. 2006, https://doi.org/10.1179/174329406X140199.

[10] K. S. Jung, "Nitriding of iron-based ternary alloys : Fe-Cr-Ti and Fe-Cr-Al," Ph.D. dissertation, University of Stuttgard, Stuttgard, Germany, 2011.

[11] Z. Pokorny, J. Kadlec, V. Hruby, Z. Joska, and D. Q. Tram, "Mechanical Properties of Steels after Plasma Nitriding Process," *Journal of Materials Science and Engineering*, vol. A, no. 1A, pp. 24–25, 2011.

[12] Y. Li and P. Gu, "Free-form surface inspection techniques state of the art review," *Computer-Aided Design*, vol. 36, no. 13, pp. 1395–1417, Nov. 2004, https://doi.org/10.1016/j.cad.2004.02.009.

[13] U. Huchel and S. Strämke, "Pulsed Plasma Nitriding of Sintered Parts – Production Experiences," *Nitrierpraxis*. http://www.nitrierpraxis.de/pulsed-plasma-nitriding-of-sintered-parts-production-experiences.

[14] D. Pye, *Practical Nitriding and Ferritic Nitrocarburizing*. ASM International, 2003.

[15] D. D. Trung, "Application of EDAS, MARCOS, TOPSIS, MOORA and PIV Methods for Multi-Criteria Decision Making in Milling Process," *Strojnícky časopis - Journal of Mechanical Engineering*, vol. 71, no. 2, pp. 69–84, Nov. 2021, https://doi.org/10.2478/scjme-2021-0019.

[16] N. V. Cuong and N. L. Khanh, "Parameter Selection to Ensure Multi-Criteria Optimization of the Taguchi Method Combined with the Data Envelopment Analysis-based Ranking Method when Milling SCM440 Steel," *Engineering, Technology & Applied Science Research*, vol. 11, no. 5, pp. 7551–7557, Oct. 2021, https://doi.org/10.48084/etasr.4315.

[17] V. C. Nguyen, T. D. Nguyen, and D. H. Tien, "Cutting Parameter Optimization in Finishing Milling of Ti-6Al-4V Titanium Alloy under MQL Condition using TOPSIS and ANOVA Analysis," *Engineering, Technology & Applied Science Research*, vol. 11, no. 1, pp. 6775–6780, Feb. 2021, https://doi.org/10.48084/etasr.4015.